

A Unified Transformer-based Network for Multimodal Emotion Recognition

Kamran Ali and Charles E. Hughes, *Member, IEEE*

Abstract—The development of transformer-based models has resulted in significant advances in addressing various vision and NLP-based research challenges. However, the progress made in transformer-based methods has not been effectively applied to biosensing research. This paper presents a novel Unified Biosensor-Vision Multi-modal Transformer-based (UBVMT) method to classify emotions in an arousal-valence space by combining a 2D representation of an ECG/PPG signal with the face information. To achieve this goal, we first investigate and compare the unimodal emotion recognition performance of three image-based representations of the ECG/PPG signal. We then present our UBVMT network which is trained to perform emotion recognition by combining the 2D image-based representation of the ECG/PPG signal and the facial expression features. Our unified transformer model consists of homogeneous transformer blocks that take as an input the 2D representation of the ECG/PPG signal and the corresponding face frame for emotion representation learning with minimal modality-specific design. Our UBVMT model is trained by reconstructing masked patches of video frames and 2D images of ECG/PPG signals, and contrastive modeling to align face and ECG/PPG data. Extensive experiments on the MAHNOB-HCI and DEAP datasets show that our Unified UBVMT-based model produces comparable results to the state-of-the-art techniques.

Index Terms—Emotion recognition, Transformers, Biosensors, Multi-model representation learning.

1 INTRODUCTION

OVER the past few years, there has been an increasing interest in adopting a bio-sensing perspective for emotion analysis. Certainly, the popularity of bio-sensing research extends beyond affective computing. Various fields such as robotics [1], [2], health [3], [4], and virtual reality [5] have also embraced bio-sensing as a valuable research tool. Bio-sensing systems, including those that measure electrocardiogram (ECG), Photoplethysmography (PPG), electroencephalogram (EEG), galvanic skin response (GSR), etc, have been available for decades; however, their size and complexity have limited their use to controlled laboratory settings and hospitals. The emergence of wearable biosensing systems has fueled the recent interest in utilizing biosensing systems for various applications by simplifying and speeding up data collection.

Several research studies have demonstrated the feasibility of recognizing human emotions through facial expressions captured in images and videos [6], [7], [8]. Although facial expression recognition systems have shown remarkable success on databases captured under controlled conditions, their performance significantly degrades [9], [10] when they are applied to real-life situations. The system's unreliability in natural environments is primarily due to various factors, such as varying head pose, illumination conditions, and occlusion of different parts of the face. Additionally, recognizing emotions from facial expressions may not be entirely dependable since they can be easily concealed or manipulated. Furthermore, facial expressions can

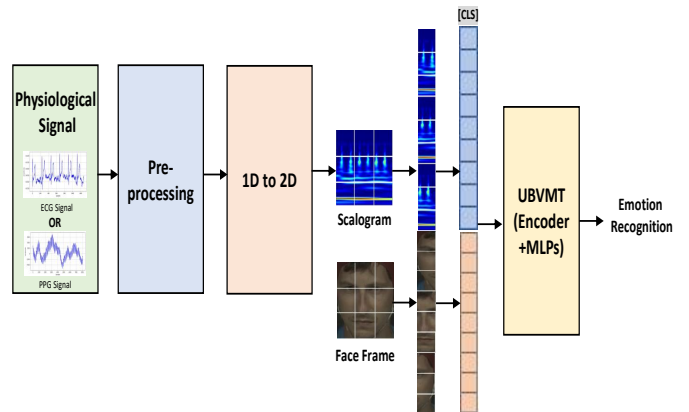


Fig. 1. The framework of UBVMT-based multimodal emotion recognition

be influenced by social and cultural differences, as human expressiveness varies among individuals. In contrast, physiological signals offer a more accurate reflection of emotions and their subtle changes. Therefore, multimodal emotion recognition techniques that combine facial information with physiological data have the potential to compensate for the drawbacks of unimodal methods and achieve more precise recognition outcomes [11], [12].

Many emotion recognition techniques have been proposed in the past years combining different modalities. For instance, in [13] Shang et al. recognized emotions by fusing EEG, EOG, and EMG signals. Similarly, in [14], Miranda et al. combined EEG, ECG, and GSR modalities to perform emotion analysis. In [15], Koelstra et al. classified emotions along the valence and arousal axes by leveraging face information and EEG signals. Most of these multimodal emotion recognition methods combine different modalities with the

• Kamran Ali and Charles E. Hughes are both with the Department of Computer Science, University of Central Florida, USA, Orlando, FL 32816.
E-mail: kamran.ali@ucf.edu

Manuscript received April 19, 2005; revised August 26, 2015.

EEG signal. However, several research studies show that there is a strong correlation between features extracted from the ECG signal and human emotions. For instance, in [16], Hany et al. extracted ECG features that represent the statistical distribution of dominant frequencies by applying spectrogram analysis to classify emotions. Similarly, in [17], time and frequency domain features are extracted from the ECG signal to perform emotion analysis. Building on those approaches, this paper presents a novel multimodal emotion recognition technique that fuses information from face video frames and ECG/PPG data. To the best of our knowledge, this is the first study that investigates the fusion of face information with the ECG/PPG signal to classify emotions.

Many attempts have been made to create effective techniques for integrating multimodal information. Initially, methods involved simply combining high-level features from all modalities to predict outcomes (known as “early fusion”) or adding up decisions made by each unimodal system with learnable weights (called “late fusion”) to produce the final inference. While these methods outperformed unimodal techniques to some extent, the lack of inter-modality interactions during training limited the potential improvement. In recent times, Transformers [18] have emerged as a highly successful approach for multimodal representation learning. Due to the advances in attention mechanisms and transformers, later studies have focused predominantly on using these techniques to develop more sophisticated multimodal fusion methods [19], [20], [21], [22], [23]. However, most of these transformer-based multimodal emotion recognition techniques leverage video, audio, and text modalities to learn joint emotion representation. In this paper, we present a unified transformer-based model that employs ECG/PPG data along with face information to recognize emotions. The main framework of the proposed method is shown in Figure 1. Based on our literature survey, no previous work has investigated the application of transformers in learning emotion representation by using face and ECG/PPG modalities.

Inspired by the compact architecture of the recently published Textless Vision-Language Transformer (TVLT) [22], we present a Unified Biosensor-Vision Multimodal Transformer (UBVMT) network to recognize emotions by fusing face and ECG/PPG data. We first investigated the effectiveness of various image-based representations of ECG/PPG signals for biosensor-based unimodal emotion recognition. Several previous methods have employed an image-based representation of an ECG/PPG signal for heart rate estimation [24], [25], [26], [27], [28]. For instance, in [24], Song et al. obtained a spatiotemporal representation of a pulse signal in a time-delayed way by constructing a Toeplitz matrix. The Toeplitz matrix is then converted into an image that is fed to a CNN to estimate heart rate information. The simplicity of the Toeplitz representation allows it to preserve both the morphological and chronological details of the 1D pulse signal. As a result, the CNN can accurately extract the correct HR values from input feature images.

In [25], average pooling is applied to various blocks within an ROI region. The spatiotemporal maps are then generated by arranging these temporal sequences into rows, which are then fed to a deep network to get HR values. In [26], the sample mean sequences of the R, G, and B

channels from the ROI of videos are extracted, and Short-Time Fourier Transform (STFT) is applied to construct the 2D time-frequency representations of the sequences. In [27], a spatiotemporal map is first computed from the input video as a representation of the BVP signal, and the spatiotemporal images are then mapped to BVP signals using the generative adversarial learning technique. In [28], Khare et al. converted the time-domain EEG biosignals into a time-frequency representation by employing Smoothed Pseudo Wigner-Ville distribution (SPWVD).

Apart from the image-based representation of ECG signals for heart rate estimation, some works [29] and [30] have extracted deep learning features from the scalogram of biosensor signals to recognize cognitive load and hypertension risk stratification, respectively. They converted the PPG signals to Scalograms by using Continuous Wavelet Transform. Scalograms were used instead of spectrograms as the image representation for PPG signals. This is because scalograms provide better highlighting of the low-frequency or rapidly changing frequency components of the signal as compared to spectrograms.

In this paper, we first investigate and compare the performance of three image representations of the ECG/PPG signal for emotion recognition. More specifically, we perform unimodal emotion recognition by converting the time domain ECG/PPG signal into 1. spatiotemporal maps [24], 2. time-frequency representation by employing Smoothed Pseudo Wigner-Ville distribution (SPWVD) [28], and 3. Scalograms [29] [30]. We show that the best emotion recognition performance is obtained by employing the scalogram representation of the ECG and PPG signals. Therefore, our Unified Biosensor-Vision Multimodal Transformer (UBVMT) network is trained and validated by using the scalogram representation of the ECG/PPG signal along with the face images. The effectiveness of the proposed UBVMT-based multimodal emotion recognition technique is validated on two datasets: the MAHNOB-HCI [31] and DEAP [32] datasets. Extensive experiments show that the proposed approach produces comparable results to the state-of-the-art emotion recognition techniques. Overall, the main contributions of this paper are as follows:

- Comparison of the performance of three image-based representations, namely spatiotemporal maps, time-frequency representation, and scalograms of the ECG/PPG signal for emotion recognition, and evidence that scalograms better represent the emotion features contained by the ECG/PPG signals.
- A novel technique that employs transformer architecture for biosensor-based multimodal emotion recognition.
- The Unified Biosensor-Vision Multimodal Transformer (UBVMT) network consisting of homogenous blocks that learn vision-and-biosensor emotion representation with minimal modality-specific design, thus, making it compact and applicable in real-time emotion analysis.
- Experimental results showing that the proposed Unified Biosensor-Vision Multimodal Transformer-based (UBVMT) technique learns effective multimodal emotion representation by fusing face with

ECG/PPG data.

- A baseline for emotion recognition research created by the fusion of face data with an ECG/PPG signal.

2 RELATED WORK

Psychologically, human emotions can be characterized based on two main frameworks: categorical or dimensional representations. In the categorical framework of emotions, emotions are classified into distinct labels such as joy, sadness, anger, happiness, fear, and so on. This approach considers emotions as discrete categories rather than continuous dimensions. In dimensional conceptualizations of emotions, a commonly used framework involves representing emotions within a two-dimensional space. In this space, valence is positioned along one axis, while arousal is positioned along the other [33]. Valence, often positioned on the horizontal axis, signifies the extent of pleasantness or unpleasantness. On the other hand, arousal, typically placed on the vertical axis, represents the level of activation or energy associated with the emotion. Within a two-dimensional (2D) space, as shown in Figure 2, emotions are portrayed by their valence and arousal level. While the categorical approach to emotions is conceptually straightforward, it faces certain challenges. It struggles to represent compound emotions that do not fit neatly into a single category, and it does not provide a means to quantify the degree or intensity of an emotional state. Therefore, in this paper, a novel multimodal emotion recognition technique is developed to classify emotions along the valence-arousal axis.

2.1 Emotion Recognition with ECG/PPG Signals

Previous research shows that there is a strong correlation between ECG/PPG signals and human emotion. In [34], Yu et al. converted the rPPG signal of an input image into time-frequency domain spectrogram images to classify the short-term emotions. In [35], Ismail et al. employed ECG and PPG signals to develop an emotion recognition system, and compared the performance of both signals for classifying emotions. Lee et al. in [36] investigated the ability of PPG signals to recognize emotions along the arousal-valence axis. Sepúlveda et al. in [37] performed emotion recognition from ECG signals using a wavelet scattering algorithm. Emotion features of the ECG signal are extracted at different time scales leveraging the wavelet scattering technique, and the extracted features are then fed into different classifiers to perform emotion analysis. Sarkar et al. in [38] exploited a self-supervised deep multi-task learning framework to develop an emotion recognition algorithm using the ECG signals. Mellouk et al. presented a rPPG signal-based emotion classification method using a deep learning architecture, which combines a one-dimensional convolution neural network (1DCNN) and a long short-term memory (LSTM) [39]. In [16], Ferdinando et al. extracted emotion features from ECG signals using spectrogram analysis of intrinsic mode function after applying the bivariate empirical mode decomposition to ECG. Similarly, in [17], Ferdinando et al. derived heart rate variability (HRV) features from ECG signals to categorize emotions in an arousal-valence space. In [29], Gasparini et al. used a scalogram-based representation

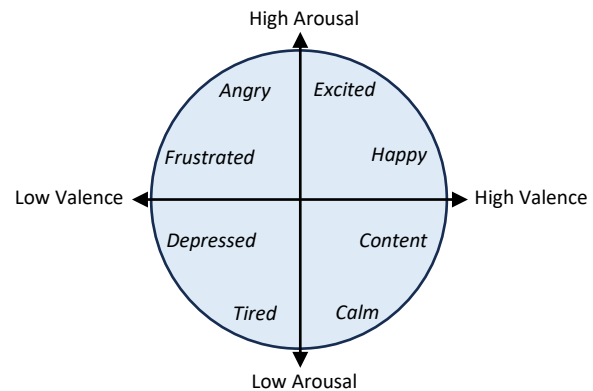


Fig. 2. Arousal valence emotion model

of a PPG signal to extract deep learning features for the recognition of cognitive load. Gasparini et al. showed that the deep learning features outperformed hand-crafted features to classify cognitive load, especially by leveraging feature selection methods to avoid the curse of dimensionality. Similarly, Liang et al. in [30], converted the PPG signals into scalogram-based representations using continuous wavelet transforms that are input to a deep learning method for the classification and evaluation of hypertension.

2.2 Emotion Recognition with Facial Images

Facial images and videos have been widely used by the research community to recognize emotions. Mostly, facial information is used to analyze emotions by using facial expression recognition techniques [40], [41], [42], [43], [44]. However, in this paper, a transformer-based technique is presented that estimates the continuous dimensions related to emotions. Based on the dimensional approach, affective behavior can be characterized using various underlying continuous dimensions. These dimensions offer a more accurate representation of the emotions individuals experience in their daily lives. As noted in Figure 2, two widely utilized dimensions are valence, which reflects the positivity or negativity of an emotional state, and arousal, which gauges the intensity of emotional activation [45], [46], [47].

To estimate valence and arousal from facial images, Dimitrios et al. [48] used a Convolutional and Recurrent (CNN-RNN) deep neural architecture to extract emotion features for dimensional emotion recognition. Deng et al. [49] used the ResNet-50 model for multi-task expression recognition and implemented the teacher-student architecture to enhance the training data without labels. This approach aims to address the imbalanced data distribution across different tasks. In [50], Kuhnke et al. utilized facial landmarks to align the image and eliminate conflicting data. They achieve this by leveraging the correlation among different representations to generate pseudo-labels. In [51], the features extracted from a 3D-CNN are inputted into the 3D VGG and 2D SENet-101 networks. Subsequently, Gated Recurrent Units (GRUs) are employed to enhance the model's ability to learn temporal features.

2.3 Multi-modal Emotion Recognition

There have been many studies focusing on the analysis of multimodal systems for recognizing human emotions.

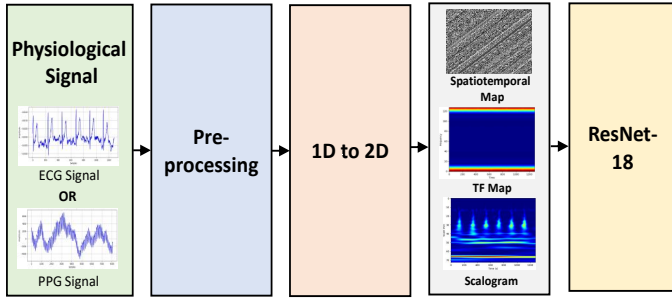


Fig. 3. Unimodal emotion recognition

These studies have demonstrated that, by integrating information from multiple modalities, the performance of models for recognizing emotions can be enhanced [52]. Therefore, in [53], Yin et al. fused information from ECG signal with Electroencephalogram (EEG), Electrooculography (EOG), Galvanic Skin Response (GSR), Electromyography (EMG), skin temperature, blood volume, and respiration to recognize emotions. Miranda et al. [14] recorded EEG, GRS, and ECG signals using wearable sensors and combined EEG and GRS information with the ECG signal to categorize human emotions. Soleymani et al. [31] employed Hidden Markov Models (HMMs) to classify emotions by integrating ECG features with EEG, GSR, respiration, and skin temperature data. In [54], Stamos et al. fused emotion features extracted from the ECG signal with the features obtained from the EEG signal to perform emotion analysis. Santamaria et al. [55] integrated the modalities of ECG and GSR to recognize emotions by employing Deep Convolutional Network (DCNN). Elalamy [56] performed emotion analysis using the spectrogram and recurrence plots (RP) of ECG, EDA, and Photoplethysmography (PPG) signals individually, and investigated the performance by combining this information for multi-modal emotion recognition. Most of the aforementioned techniques fuse the ECG signal with other modalities such as EEG, EMG, GSR, etc., for multi-modal emotion analysis. But, unlike the EEG signal, which has been combined with the facial information as proposed in [15], [57], [58], the ECG signal has not been fused with facial features to perform emotion recognition. In this paper, a Unified Biosensor-Vision Multimodal Transformer-based (UBVMT) emotion recognition technique is presented that integrates ECG/PPG data with facial information.

3 RESEARCH METHODS

This section discusses various 1D-to-2D transformation methods to extract emotion features from 2D representation of ECG/PPG signals. We then present our Unified Biosensor-Vision Multimodal Transformer (UBVMT) architecture that leverages the 2D representation of ECG/PPG signals along with face information to recognize emotions.

3.1 The 2D Representation of ECG/PPG Signals

In this paper, one of our goals is to find an effective method that can be used to transform the 1D time domain signal of ECG/PPG data into an image-based representation for emotion recognition. Therefore, in this section, we investigate the effectiveness of three different 1D-to-2D transformation

techniques to perform 2D image-based emotion analysis using ECG/PPG data. More specifically, we present a unimodal emotion recognition network using ResNet-18 [62] by converting the time domain ECG and PPG signals into (1) spatiotemporal maps [24], (2) time-frequency representation by employing Smoothed Pseudo Wigner-Ville distribution (SPWVD) [28], and (3) Scalograms [29], [30] as shown in Figure 3.

3.1.1 Spatiotemporal Representation of ECG/PPG signal

In this section, a novel emotion recognition technique using a spatiotemporal representation of an ECG/PPG signal is presented. Rencheng et al. [24] converted a 1D ECG and PPG signal into a 2D spatiotemporal map to estimate heart rate information. It has been reported that the performance degradation of the conventional PPG signals for heart rate estimation due to noise can be overcome by employing deep learning techniques on the spatiotemporal maps of the PPG signal [24]. Therefore, in this section, we apply the technique proposed in [24] to convert the 1D ECG/PPG signal into a 2D spatiotemporal map and perform emotion analysis using the spatiotemporal maps as input to the classifier. The spatiotemporal feature maps can retain both the morphological and chronological features of ECG/PPG signals.

Construction of ECG/PPG Spatiotemporal Map: The spatiotemporal feature map of an ECG/PPG signal is constructed by creating a square Toeplitz matrix. Suppose the 1D input signal $S = (s_1, s_2, \dots, s_P)$ has P samples and P is an even number. The first row of the matrix consists of s_1 to $s_{P/2}$ samples. Similarly, the second row contains samples from the second point, i.e., s_2 to the $(P/2 + 1)$ th sample, and so on. Therefore, a square Toeplitz matrix T with a size equal to $P/2$ is constructed as:

$$T = \begin{bmatrix} s_1 & s_2 & \dots & s_{P/2} \\ s_2 & s_3 & \dots & s_{P/2+1} \\ \cdot & \cdot & \cdot & \cdot \\ \cdot & \cdot & \cdot & \cdot \\ \cdot & \cdot & \cdot & \cdot \\ s_{P/2} & s_{P/2+1} & \dots & s_{P-1} \end{bmatrix}$$

A gray image is constructed by converting the matrix T into an image representation. The obtained gray image has a clear structure because the input signal is quasiperiodic. The second row of Figure 4 shows the spatiotemporal image representation of 1D signals. As it can be seen in Figure 4 that the vertical patterns preserve the period information of the 1D signal. This suggests that the 2D Toeplitz representation can effectively capture and portray the periodic nature of a 1D signal. The morphological and chronological information of the 1D signal is preserved in this simple 2D spatiotemporal representation. Therefore, emotion features can be extracted from these 2D maps of the ECG/PPG signals. The spatiotemporal image representations of ECG/PPG signals were then adjusted to the size of $224 \times 224 \times 3$, and fed to a pre-trained ResNet-18 [62] to perform emotion analysis.

3.1.2 Time-frequency Representation of ECG/PPG Signal

To leverage the effectiveness of Convolutional Neural Networks (CNNs), Khare et al. [28] converted 1D EEG signals

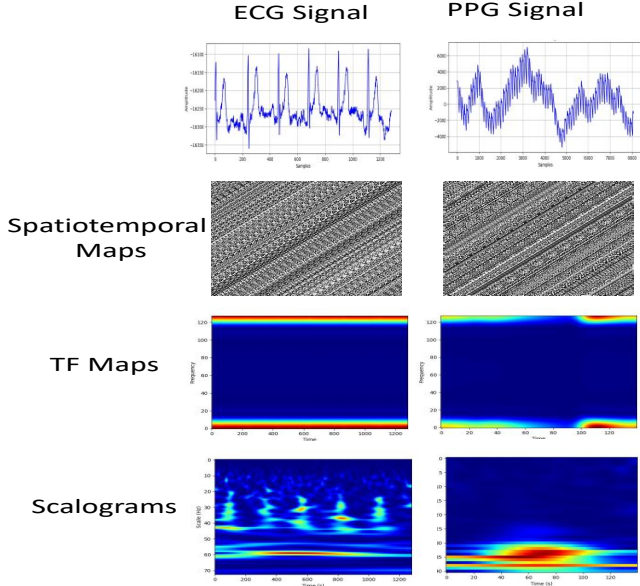


Fig. 4. 2D representations of ECG/PPG signal

into 2D maps using a Time–Frequency (TF) representation for emotion recognition. More specifically, filtered EEG time-domain signal is transformed into time, frequency, and amplitude representation by employing Smoothed Pseudo-Wigner–Ville Distribution (SPWVD). The transformation of time-domain signals into Time-Frequency (TF) representation enables the preservation of signal information in the spectral domain. TF map is a representation that combines time, frequency, and amplitude in a spatial format simultaneously. Therefore, a time-frequency representation of the ECG/PPG signal can also be obtained by using other time-frequency analysis techniques such as Short-Time Fourier Transform (STFT), Wigner–Ville distribution, and so on. The time-frequency representation obtained by using STFT is known as a spectrogram. To perform Short-Time Fourier Transform (STFT), certain parameters need to be defined, such as the window size, shape, and sampling frequency. It is crucial to maintain a consistent window length across the entire signal. However, the resulting spectrogram from STFT often exhibits limited resolution due to the trade-off between time and frequency localization. In contrast, the utilization of the Wigner–Ville distribution for obtaining the time-frequency representation results in the presence of cross-terms and attenuation for low frequencies. As reported in [59], SPWVD offers enhanced time-frequency resolution, effectively resolving the limitations associated with STFT. The challenges associated with the Wigner–Ville distribution are tackled in SPWVD by incorporating a cross-term reducing window in the frequency domain.

In this paper, one of our goals is to find an effective method that can be used to transform the 1D time domain signal of ECG/PPG into an image-based representation. Therefore, to address the aforementioned constraints of STFT and the Wigner–Ville distribution, in this section, the technique of Smoothed Pseudo-Wigner–Ville Distribution (SPWVD) is employed to convert time-domain ECG/PPG signals into a time-frequency representation. The performance of a SPWVD-based TF representation of ECG/PPG signals is then investigated for emotion

recognition.

Construction of ECG/PPG TF Map: SPWVD provides a straightforward depiction of the localization of signal energy in both time and frequency domains. The choice of the length and type of the cross-term reducing window in both the time and frequency domains can be made independently. Due to the independent selection of the length and type of the cross-term reducing window, SPWVD exhibits favorable time-frequency cluster characteristics. The representation of SPWVD in mathematical terms can be expressed as [59], [60].

$$SPWVD(t, f) = \int_{t_1} \int_{f_1} u(t - t_1)v(f - f_1)W(t_1, f_1), dt_1 df_1 \quad (1)$$

$$W(t, f) = \int_{-\infty}^{\infty} x(t + \frac{\tau}{2})x^*(t - \frac{\tau}{2})e^{-j2\pi f\tau} d\tau \quad (2)$$

where $u(t)$ represents the smoothing window in the time domain, $v(f)$ denotes the smoothing window in the frequency domain, τ corresponds to a lag, and $x(t)$ is the input signal. Controlling the smoothing scales in both the time and frequency domains is straightforward. The length of the windows for $u(t)$ and $v(f)$ can be chosen independently. The TF representation of time-domain ECG/PPG signals obtained by employing the SPWVD technique is shown in the third row of Figure 4.

To mitigate cross-terms in both time and frequency domains, the Kaiser window is employed. However, selecting a window size that is too small may lead to diminished resolution, while overly large windows can significantly increase the image size. Consequently, a medium-sized window with a length of 31, as suggested in [28], is chosen. For efficient computation, the window size is maintained at $2^n - 1$, where n represents the number of bits. The TF representations of time-domain ECG/PPG signals are then adjusted to the size of $224 \times 224 \times 3$, and fed to a pre-trained ResNet-18 [62] to perform emotion recognition.

3.1.3 Scalogram of ECG/PPG Signal

Gasparini et al. [29] converted the monodimensional photoplethysmography (PPG) data into a bidimensional representation, and applied a pre-trained CNN to classify the different levels of the subject’s hypertension. More specifically, the 1D PPG signals were converted into scalograms by leveraging Continuous Wavelet Transform [61]. Gasparini et al. opted to utilize the scalogram instead of the spectrogram as the image representation for PPG signals. The reason for this choice is that scalograms offer enhanced highlighting of low-frequency or rapidly changing frequency components in the signal, compared to spectrograms. Similarly, in [30], Liang et al. converted 1D PPG signals into 2D scalograms by using Continuous Wavelet Transform to classify hypertension. In this paper, we investigate the performance of scalogram representation of ECG/PPG signals for deep learning-based emotion recognition.

Construction of ECG/PPG scalograms: Continuous Wavelet Transform (CWT) has been used for decades as a valuable technique for analyzing both time and frequency information. In this paper, each segment of the ECG/PPG signal was transformed into a time-frequency representation, known as a scalogram, using the continuous wavelet transform method. A scalogram represents the absolute values of the continuous wavelet transform coefficients of a signal, displayed as a graph of time and frequency. In contrast to a spectrogram, a scalogram provides improved capability in identifying the low-frequency or rapidly changing frequency components of the signal. To convert the PPG signal into a scalogram, we obtained the absolute values of the wavelet coefficients for each signal segment using the analytic morse (3,60) wavelet. The scalogram representation of ECG/PPG signals obtained by employing the CWT technique is shown in the fourth row of Figure 4. The scalograms were then adjusted to the size of $224 \times 224 \times 3$, and fed to a pre-trained ResNet-18 [62] to perform emotion recognition.

3.2 The Unified Transformer-based Multi-modal Network

In this section, we discuss our Unified Biosensor-Vision Multimodal Transformer (UBVMT) network where homogeneous transformer blocks take 2D representations of ECG/PPG signals and raw visual inputs for multi-modal emotion representation learning with minimal modality-specific design. UBVMT is trained by employing masked autoencoding [63] and contrastive modeling [22] to learn effective emotion representation. The overall architecture of our Unified Biosensor-Vision Multi-modal Transformer (UBVMT) network is shown in Figure 5. The objective of masked autoencoding is to reconstruct masked patches of 2D representations of ECG/PPG signals and face video frames, while contrastive modeling is applied to align ECG/PPG and face information. We argue that, due to the unified architecture of UBVMT, the computational redundancy and complexity of our method is reduced as compared to conventional transformer-based multi-modal emotion recognition techniques.

The input to the UBVMT is the integration of face patch embedding, ECG/PPG patch embedding, and modality embedding. To obtain face embeddings, the face image of $224 \times 224 \times 3$ pixels is divided into a list of 16×16 sized patches. The pixel values of each patch are normalized, and a linear projection layer is used to convert face patches into a 768-dimensional patch embedding. For an input face image of size $224 \times 224 \times 3$, the size of the resultant face embedding is 14×14 . The spatial embedding involves incorporating spatial information for each input patch by adding a distinct trainable vector to the height and width axes of the 14×14 embeddings. For ECG/PPG embedding, the 2D representation of an ECG/PPG signal is divided into patches, and a linear projection layer is applied on each patch to obtain a 768-dimensional patch embedding. Similar to the face modality, a patch size of 16×16 is used, and trainable temporal and frequency embeddings are utilized to denote the temporal and frequency information of the patches.

3.2.1 The architecture of UBVMT

Similar to the transformer model proposed in [18], UBVMT has an encoder E which has 12 layers (hidden size 768), and a decoder D with 8 layers (hidden size 512). After pretraining, we only employ the encoder E part of the transformer and finetune it for emotion recognition.

3.2.2 Pretraining UBVMT

UBVMT is pre-trained by employing masked autoencoding [63] and contrastive modeling [22] to learn effective emotion representation. The pretraining objective function \mathcal{L} is the weighted sum of masked autoencoding loss \mathcal{L}_M and the contrastive modeling loss \mathcal{L}_C :

$$\mathcal{L} = \lambda_M \mathcal{L}_M + \lambda_C \mathcal{L}_C \quad (3)$$

where $\lambda_M = 0.4$ and $\lambda_C = 1$.

Masked Autoencoding Objective Function: The main objective of masked autoencoding is to learn effective unimodal representations in biosensor-and-vision settings. This objective involves masking random patches of ECG/PPG images and the face video frames, allowing us to reconstruct missing inputs effectively. Specifically, we implement a random dropout mechanism on a portion of ECG/PPG embedding x^B and face embedding x^F . Subsequently, we input the remaining patch embeddings to the encoder E . To generate the input to the decoder D , we add the dropped embeddings as trainable vectors labeled as [MASK] and position them in the same locations as the original inputs (indicated by gray boxes in Figure 5. Additionally, the corresponding positional, and frequency embeddings, which are separately parametrized, are incorporated into the decoder input. The objective function of masked autoencoding is a mean squared error between the reconstructed and original ECG/PPG images and face video frames:

$$\mathcal{L}_M = \frac{1}{N_m^B} \sum_{i \in \text{masked}} \|x_i^B - \hat{x}_i^B\|_2^2 + \frac{1}{N_m^F} \sum_{j \in \text{masked}} \|x_j^F - \hat{x}_j^F\|_2^2 \quad (4)$$

where N_m^B and N_m^F are the number of masked patches for ECG/PPG images and face video frames, respectively. Loss \mathcal{L}_M is computed only on masked patches. Note that the ECG/PPG and face output of the encoder are fed to the decoder separately.

Contrastive Modeling Objective Function: The main objective of contrastive modeling is to perform ECG/PPG-vision matching and learn an effective cross-modal representation, as shown in Figure 5. For every face image, a positive vision-ECG/PPG pair $(x^{F+}; x^B)$ is generated. Additionally, we form half of the vision-ECG/PPG pairs within a batch as mismatched (negative) pairs $(x^{F-}; x^B)$ by substituting the face images x^{F+} with randomly selected face images x^{F-} from the training dataset.

Similar to previous multimodal transformers [22], [64], [65], [66], [67], we incorporate a linear layer with sigmoid activation as the classification head. This is applied to the encoder output of the first [CLS] token, resulting in the matching probability p by employing binary cross-entropy loss:

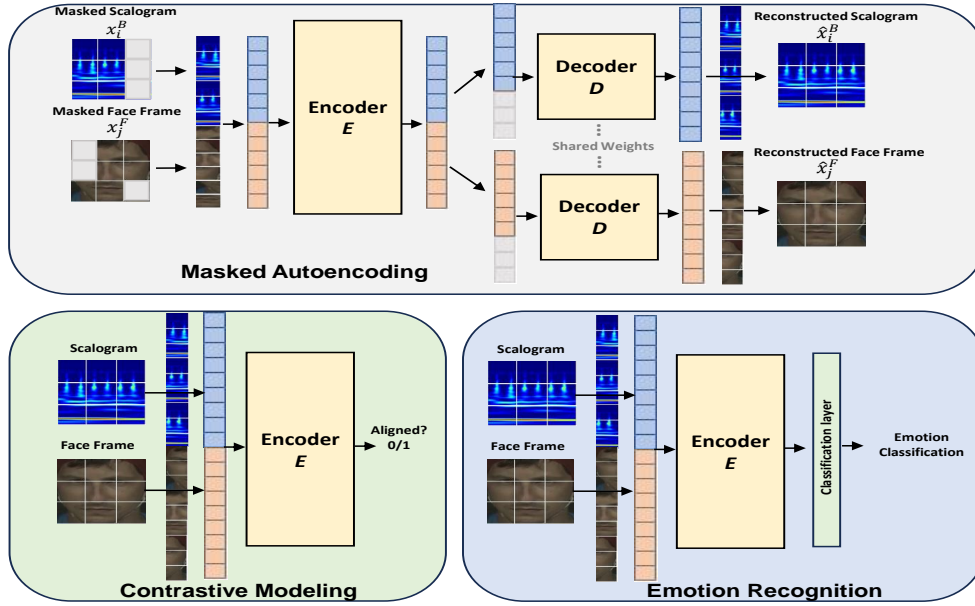


Fig. 5. Multimodal emotion recognition

$$\mathcal{L}_C = -y \log p \quad (5)$$

where the value of y is set to 1 when the input vision-ECG/PPG pair $(x^F; x^B)$ is positive (match), and 0 otherwise. Throughout the training process, \mathcal{L}_M and \mathcal{L}_C are computed using separate forward passes.

4 EXPERIMENTAL DETAILS

4.1 Database Description

The effectiveness of transformer models to learn multimodal representation is improved by pretraining them on large datasets [65], [66], [67]. As such, UBVMt is pre-trained on the large, comprehensive CMU-MOSEI [68] dataset. Similar to [24], [25], [69], rPPG signals are extracted from the CMU-MOSEI video clips using the MTTs-CAN [70] method. After pertaining, MAHNOB-HCI [31] and DEAP [32] datasets are used for multimodal emotion analysis.

The **CMU-MOSEI** dataset comprises 23,454 movie review clips, totaling over 65.9 hours of YouTube video content. It features contributions from 1000 speakers and encompasses 250 distinct topics. Videos having non-human faces and faces with more than 80° head rotations from the frontal position are discarded from the dataset. From each video, multiple video clips of 1.1 secs are extracted, with the number of clips being dependent on the length of each video. For our case, 90,037 video clips are extracted from the entire CMU-MOSEI dataset. These video clips are then fed to the MTTs-CAN [70], and only the pulse signals from the MTTs-CAN are used to obtain the rPPG signals of these video clips.

The **MAHNOB-HCI** [31] (Multimodal Human-Computer Interaction) dataset is a widely used publicly available dataset designed for research in affective computing and multimodal emotion recognition. The dataset includes 527 facial video recordings of 27 participants engaged in various tasks and interactions, while their physiological signals such as 32-channel electroencephalogram (EEG), 3-channel electrocardiogram

(ECG), 1-channel galvanic skin response (GSR), and facial expressions are captured. The ECG signals were sampled at a rate of 256 Hz. The ECG data is precisely synchronized and aligned with the face video recordings. Similar to [71], only the EXG2 signal from the 3 ECG channel system is extracted for emotion analysis.

The Database for Emotion Analysis using Physiological Signals (**DEAP**) [32] is a widely used and publicly available database designed for research in emotion analysis and affective computing. The DEAP database contains data from 32 participants, aged between 19 and 37 (50% female), who were recorded watching 40 one-minute music videos. Each participant was asked to evaluate each video by assigning values from 1 to 9 for arousal, valence, dominance, like/dislike, and familiarity. Face video was recorded for 22 out of the 32 participants, and the proposed UBVMt method is evaluated using this particular group of subjects. For each dataset, we conduct a subject-independent 10-fold cross-validation evaluation.

4.2 Pre-processing Steps

The MAHNOB-HCI emotion elicitation data contains unstimulated baseline and stimulated response ECG signals. Furthermore, the database includes a synchronization signal that facilitates the separation of the two. Our experiments exclusively utilized the ECG signals recorded during the stimulated phase. To remove motion artifacts, the original signal is subtracted by the smoothing signal [31]. Subsequently, similar to [16], [17] a notch filter was applied at 60 Hz to eliminate power line interference. Baseline drift was mitigated by implementing a highpass filter at 0.4 Hz. Additionally, other noises were eliminated using a low-pass filter set at 200 Hz. Due to the variability in the length of the ECG signals, they are partitioned into segments of 5 seconds each.

The PPG and rPPG signals from the DEAP and CMU-MOSEI datasets are preprocessed and segmented into segments of pulses corresponding to 1.1 secs following [36].

PPG signal can be affected by disturbances, such as movement at the sensor attachment site. Consequently, PPG signals in the DEAP dataset contain movement noise. Hence, before segmenting PPG signals into single pulses of 1.1 secs, a high-order polynomial (an order of 50 polynomials) is fitted to the PPG signal. Subsequently, the fitted curve is subtracted from the original PPG signal, effectively eliminating any movement noise. To partition the PPG signal into single pulses of 1.1 secs, we first find the maximum or peaks of the signal and then use the peak value as the center of the segmenting window. The next pulse is segmented by moving the center of the segmenting window to the next peak, and so on. The biosignal data vary from person to person; as such, the PPG/rPPG signals are normalized to mitigate variations in PPG signal size among individuals. We must exercise caution to retain the personal characteristics of the signal, as they vary depending on the emotions. The PPG signals are normalized by employing personal maximum and minimum [36]:

$$\bar{z}_i = \frac{(z_i - \min_{person})}{(\max_{person} - \min_{person})} \times \alpha \quad (6)$$

where z_i is the PPG signal, \bar{z}_i is the normalized signal, and α is set to 1000 to normalize z_i between 0 to 1000. After extracting the signal segments and their corresponding video frames, we balance the dataset by discarding some segments that contain neutral facial expressions. We employ the off-the-shelf TER-GAN [6] FER model trained on the in-the-wild AffectNet [10] dataset to detect segments containing non-neutral facial expressions.

4.3 Unimodal Emotion Recognition Details

This section presents the experimental details of the unimodal emotion recognition experiments that were performed to investigate and compare the performance of the three 2D representations of ECG/PPG signals. These experiments were conducted by inputting only the 2D image-based representations of the ECG signal (in the case of MAHNOB-HCI dataset), and the PPG signal (in the case of DEAP dataset) to a pre-trained ResNet-18 [62]. ResNet-18 was employed to classify emotions in an arousal-valence space using both the MAHNOB-HCI and DEAP datasets. In the case of the MAHNOB-HCI dataset, the arousal dimension consisted of three categories: ‘calm’, ‘medium’, and ‘activated’, while the valence dimension included the categories ‘unpleasant’, ‘neutral’, and ‘pleasant’, similar to the class distribution presented in [17]. The arousal and valence classes in the DEAP dataset are annotated on a 1-9 scale. Therefore, following [36], the arousal and valence are split into two binary classes based on a threshold of 5, indicating high and low arousal, and high and low valence, respectively.

ResNet-18 is finetuned by using Adam [72] optimization algorithm with a learning rate of 0.001, batch size of 128, and cross-entropy loss function. The ResNet-18 is trained for 50 epochs, and 10-fold cross-validation is employed for the evaluation of the 2D ECG/PPG representation-based unimodal emotion recognition technique. The best emotion recognition performance is obtained by converting 1D ECG

TABLE 1
MAHNOB-HCI dataset: Performance comparison of 2D representations of ECG signal for unimodal emotion recognition.

Method	Valance	Arousal
Spatio-temporal maps [24]	37.62	41.04
SPWVD [28]	38.39	42.75
Scalogram [29], [30]	42.91	49.14

TABLE 2
DEAP dataset: Performance comparison of 2D representations of PPG signal for unimodal emotion recognition.

Method	Valance	Arousal
Spatio-temporal maps [24]	60.26	62.71
SPWVD [28]	64.03	65.19
Scalogram [29], [30]	76.51	77.02

and PPG signals into the 2D scalogram representation. Further details and comparison of the performance of the three 2D representation techniques are discussed in section 5.1.

4.4 Multimodal Emotion Recognition Details

Multimodal emotion recognition is performed by applying our novel Unified Biosensor-Vision Multi-modal Transformer (UBVMT) network for emotion recognition in an arousal-valence space using the facial expression information and 2D representation of ECG/PPG data from the MAHNOB-HCI and DEAP datasets, respectively. As far as we are aware, we are the first ones to model the co-relation between the face and ECG/PPG data for emotion recognition employing a transformer network. For the extraction of the face information, since the ECG and PPG signals are synchronized with the facial videos of the participants in both datasets, we partitioned the videos into clips of 5 secs for the MAHNOB-HCI dataset and 1.1 secs for the DEAP database. Subsequently, following [7], we extract the first frame from each video clip, pass it to MTCNN [77] to extract only the face region as a facial expression representation, and input it to the UBVMT network along with the 2D representation of the corresponding ECG/PPG signal. As mentioned in section 4.3, the best unimodal emotion recognition performance is obtained by transforming the 1D ECG and PPG signals into a 2D scalogram representation. Therefore, multimodal emotion analysis is performed by combining the facial expression images with the scalograms of ECG and PPG signals using our proposed UBVMT network.

UBVMT is trained using the Adam [72] optimizer, with a batch size of 4, learning rate of 1e-4, and using a cosine schedule [73] with a decay rate set at 0.001. To formulate the pretraining objective in equation 3, the values of λ_M and λ_C are set to 0.4 and 1, respectively. Following MAE [63] and TVLT [22], a random masking strategy is applied, where 75% of the face and ECG/PPG patches are randomly masked. After pretraining, the encoder of UBVMT is detached, and a two-layer MLP is added on top of the encoder representation for emotion analysis. The encoder plus the MLP layers are fine-tuned using the Adam [72] optimizer, the learning rate of 1e-4, and a decay rate of 0.001. All the training and validation processes are carried out using dual NVIDIA Tesla V100 GPUs.

5 RESULTS AND ANALYSIS

In this section, the experimental results of both the unimodal emotion recognition and the multimodal emotion analysis using the proposed UBVM method are discussed in detail.

5.1 Results and Analysis of Unimodal Method

The unimodal emotion recognition performance of the three 2D representations of ECG/PPG signals for MAHNOB-HCI and DEAP datasets are presented in Table 1 and Table 2 as an average of the 10-fold cross-validation. As it can be seen, the scalogram representation of both ECG and PPG signals outperforms the emotion recognition performance of the spatiotemporal maps and the SPWVD-based 2D representation. The superior performance of scalogram representation is because it is more effective at identifying the low-frequency or rapidly-changing frequency components of the signal, as both ECG and PPG are low-frequency signals. Similarly, the emotion recognition accuracy of SPWVD is higher than the accuracy of spatio-temporal maps because SPWVD offers better time-frequency resolution, and thus captures emotion features more effectively than the spatio-temporal maps.

The performance of our unimodal emotion recognition method is also compared with the state-of-the-art unimodal emotion recognition techniques on both the MAHNOB-HCI and DEAP datasets, as presented in Table 3. For the MAHNOB-HCI dataset, we compare our result with the ECG-based emotion analysis technique proposed by Ferdinando et al. [17] and rPPG-based method of Yu et al. [76]. In [17], Ferdinando et al. extracted heart rate variability (HRV) features from ECG signals to classify emotions. As it can be seen in Table 3, our scalogram-based method outperforms the emotion recognition technique proposed in [17]. In [76], Yu et al. extracted ten-dimensional HRV features from rPPG signals of MAHNOB-HCI video clips, and fed them to a support vector machine for emotion classification. Table 3 shows that they achieve a higher recognition accuracy in the case of valence, while our scalogram-based method outperforms their method in arousal categorization. Similarly, in Table 3, the performance of our PPG-based emotion classification method is compared with the state-of-the-art emotion analysis techniques using the DEAP database. For the comparison of the techniques involving only the PPG signal, our 2D scalogram-based method is compared with the PPG-based technique proposed by Lee et al. [36] and various 2D representations of PPG signal employed by Elalamy et al. [56]. Table 3 shows that our scalogram-based PPG technique is more effective than the one-dimensional convolutional neural network-based (1D CNN) emotion analysis method proposed by Lee et al. [36]. Similarly, our technique produces higher recognition accuracy than the 2D spectrogram-based method proposed by Elalamy et al. [56]. Also, our 2D scalogram representation outperforms the emotion recognition performance of the Recurrence PLOT-based (RP) 2D representation technique used in [56]. Most of the physiological-based emotion analysis methods employ EEG signals for emotion recognition more than any other physiological signal due to its capability to capture emotion features more effectively. Therefore, in Table 3, we also compare our unimodal method with the state-of-the-art

TABLE 3
Performance comparison of our unimodal emotion recognition method with the state-of-the-art techniques.

Study	Modality	Valance	Arousal
MAHNOB-HCI			
Ferdinando et al. [17]	ECG	42.55	47.69
Yu et al. [76]	HRV	46.86	44.02
Our (Scalogram)	ECG	42.91	49.14
DEAP			
Patras et al. [32]	EEG	62.00	57.60
Chung et al. [74]	EEG	70.90	70.10
Campos et al. [75]	EEG	73.14	73.06
Lee et al. [36]	PPG	75.30	76.20
Elalamy et al. [56]	PPG(spectrogram)	69.60	69.30
Elalamy et al. [56]	PPG(Recurrence Plots)	69.40	69.20
Our (Scalogram)	PPG	76.51	77.02

TABLE 4
Performance comparison of our multimodal emotion recognition method with the state-of-the-art techniques.

Study	Modality	Valance	Arousal
MAHNOB-HCI			
Soleymani et al. [31]	EEG and Eye Gaze	76.10	67.70
Koelstra et al. [15]	EEG and Face	73.00	68.50
Our (UBVMT)	ECG and Face	50.01	83.84
DEAP			
Yin et al. [53]	EEG, ECG, EOG, GSR, EMG, Skin temperature, Blood volume, Respiration	76.17	77.19
Shang et al. [13]	EEG, EOG, EMG	51.20	60.90
Siddharth et al. [7]	EEG, PPG, GSR	71.87	73.05
Siddharth et al. [7]	EEG and Face	73.94	74.13
Elalamy et al. [56]	PPG, EDA	69.90	69.70
Our (UBVMT)	PPG and Face	81.53	82.64

unimodal emotion analysis techniques using EEG signals. Table 3 shows that our scalogram-based PPG representation produces higher recognition accuracy as compared to the EEG-based emotion recognition techniques of Patras et al. [32], Chung et al. [74] and Campos et al. [75]. These results imply that the scalogram-based 2D representation of the PPG signal can be used as an alternative to the EEG signal. Obtaining and utilizing EEG signals, the most prevalent bio-signal in emotion recognition, can be inconvenient due to the high cost of EEG measurement devices and the cumbersome measurement process, especially for participants from neurodiverse populations such as kids with ASD.

5.2 Results and Analysis of Multi-modal Method

The average of the 10-fold cross-validation accuracy of the UBVM multimodal emotion recognition method is

TABLE 5
F1 scores of our multimodal emotion recognition method.

Study	Dataset	Valance	Arousal
UBVMT	MAHNOB-HCI	0.501	0.846
UBVMT	DEAP	0.815	0.829

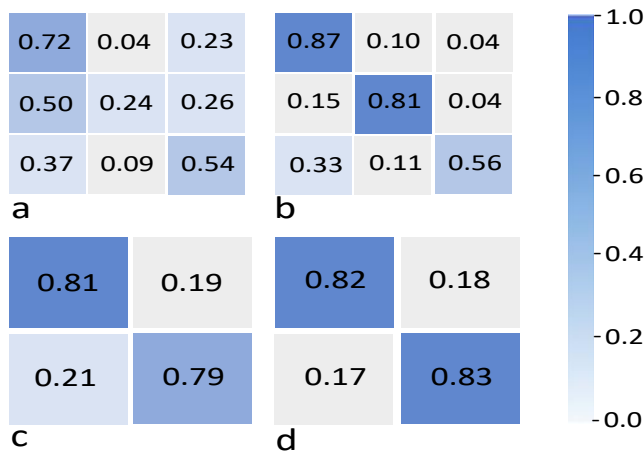


Fig. 6. The confusion matrices for (a). MAHNOB-HCI valence emotion recognition, (b). MAHNOB-HCI Arousal emotion recognition, (c). DEAP valence emotion recognition, and (d). DEAP arousal emotion recognition.

shown in Table 4. However, since our method provides a baseline for multimodal emotion recognition by fusing the ECG/PPG signal with the face information, there are no state-of-the-art methods with which we can compare our results. Nonetheless, as can be seen in Table 4 that the proposed method outperforms the multimodal techniques fusing EEG information with other physiological signals, especially for the recognition of arousal. For the MAHNOB-HCI dataset, we compare our results with the EEG-based multimodal methods proposed by Soleymani et al. [31] and Koelstra et al. [15]. Here again, the proposed method outperforms both of these techniques by a large margin in the recognition of arousal by producing an average accuracy of 83.84%. In contrast, the method proposed by Soleymani et al. [31] achieves the highest accuracy of 76.10% for the classification of the valence class. We argue that the superior performance of our technique in recognizing the arousal class is because UBVM is pre-trained by employing an rPPG signal, and it has been reported in past research that PPG signals are more effective in categorizing arousal [29]. Therefore, given a large enough ECG dataset to pre-train the UBVM network, we posit that we can improve the classification accuracy of our method for the valence class as well. For the DEAP dataset, we compare our results with the multimodal techniques fusing PPG information with other signals like EEG, EDA GSR, etc. As can be seen in Table 4, our method outperforms the state-of-the-art multimodal emotion classification techniques both in recognizing valence and arousal with average accuracies of 81.53% and 82.64%, respectively. It is interesting to note that our bimodal method outperforms the multimodal technique proposed by Yin et al. [53], where the information from EEG, ECG, EOG, GSR, EMG, Skin temperature, blood volume, and respiration signals are fused to classify emotions. Similarly, comparing our technique with the bimodal method proposed by Siddharth et al. [7] where EEG and face information are fused for emotion analysis, Table 4 shows that the fusion of PPG and face information using UBVM is more effective in recognizing emotions. Our PPG-face method is also more accurate in classifying emotions compared to the fusion of EEG, EOG, and EMG

signals [13]. In [56], similar to our approach, Elalamy et al. transformed the 1D PPG and EDA signals into 2D representations and fuse them to categorize emotions using deep networks. Table 4 shows that our scalogram-based PPG representation, when fused with the face data, produces higher recognition accuracy by employing our proposed technique. The confusion matrices and the F1 scores of the multimodal emotion recognition results are shown in Figure 6 and Table 5, respectively.

6 CONCLUSION

In this paper, a novel approach called Unified Biosensor-Vision Multi-modal Transformer-based (UBVM) method is presented to classify emotions in an arousal-valence space. The proposed technique combines a 2D representation of an ECG/PPG signal with facial information for emotion recognition. Initially, we investigated and compared the unimodal emotion recognition performance using three image-based representations of the ECG/PPG signal. Then, the Unified Biosensor-Vision Multi-modal Transformer-based network is used for emotion recognition by combining the 2D image-based representation of the ECG/PPG signal and facial information. Our unified transformer model comprises homogeneous transformer blocks that take the 2D representation of the ECG/PPG signal and associated face frame as input for emotion representation learning with minimal modality-specific design. The UBVM model is trained using a reconstruction loss involving masked patches of video frames and 2D images of ECG/PPG signals, along with contrastive modeling to align face and ECG/PPG data. Extensive experiments on the MAHNOB-HCI and DEAP datasets demonstrate that our Unified Biosensor-Vision Multi-modal Transformer-based model achieves comparable results to state-of-the-art techniques.

ACKNOWLEDGMENTS

The authors would like to thank Mustansar Fiaz, Sachin Shah, Robinson Vasquez, Lisa Dieker, Shaunn Smith, Rebecca Hines, Ilene Wilkins, Kate Ingraham, Caitlyn Bukaty, Karyn Scott, Eric Imperiale, Wilbert Padilla, Maria Demesa for the discussions and suggestions throughout this research. This research was supported in part by grants from the National Science Foundation Grants 2114808, and from the U.S. Department of Education Grants H327S210005, H327S200009. The lead author (KA) was also supported in part by the University of Central Florida's Preeminent Postdoctoral Program (P3). Any opinions, findings, conclusions, or recommendations expressed in this material are those of the authors and do not necessarily reflect the views of the sponsors.

REFERENCES

- [1] LaFleur, Karl, Kaitlin Cassidy, Alexander Doud, Kaleb Shades, Eitan Rogin, and Bin He. "Quadcopter control in three-dimensional space using a noninvasive motor imagery-based brain-computer interface." *Journal of neural engineering* 10, no. 4 (2013): 046003.
- [2] Millán, Jd R., Frederic Renkens, Josep Mourino, and Wulfram Gerstner. "Noninvasive brain-actuated control of a mobile robot by human EEG." *IEEE Transactions on biomedical Engineering* 51, no. 6 (2004): 1026-1033.

- [3] Bamidis, Panagiotis D., Christos Papadelis, Chrysoula Kourtidou-Papadeli, Costas Pappas, and Ana B. Vivas. "Affective computing in the era of contemporary neurophysiology and health informatics." *Interacting with Computers* 16, no. 4 (2004): 715-721.
- [4] Coyle, Shirley, Yanzhe Wu, King-Tong Lau, Sarah Brady, Gordon Wallace, and Dermot Diamond. "Bio-sensing textiles-wearable chemical biosensors for health monitoring." In 4th International Workshop on Wearable and Implantable Body Sensor Networks (BSN 2007) March 26–28, 2007 RWTH Aachen University, Germany, pp. 35-39. Springer Berlin Heidelberg, 2007.
- [5] Riva, Giuseppe, Fabrizia Mantovani, Claret Samantha Capideville, Alessandra Preziosa, Francesca Morganti, Daniela Villani, Andrea Gaggioli, Cristina Botella, and Mariano Alcañiz. "Affective interactions using virtual reality: the link between presence and emotions." *Cyberpsychology and behavior* 10, no. 1 (2007): 45-56.
- [6] Ali, Kamran, and Charles E. Hughes. "Facial expression recognition by using a disentangled identity-invariant expression representation." In 2020 25th International Conference on Pattern Recognition (ICPR), pp. 9460-9467. IEEE, 2021.
- [7] Jung, Tzzy-Ping, and Terrence J. Sejnowski. "Utilizing deep learning towards multi-modal bio-sensing and vision-based affective computing." *IEEE Transactions on Affective Computing* 13, no. 1 (2019): 96-107.
- [8] Fard, Ali Pourramezan, and Mohammad H. Mahoor. "Ad-corre: Adaptive correlation-based loss for facial expression recognition in the wild." *IEEE Access* 10 (2022): 26756-26768.
- [9] Kollias, Dimitrios, and Stefanos Zafeiriou. "Exploiting multi-cnn features in cnn-rnn based dimensional emotion recognition on the omg in-the-wild dataset." *IEEE Transactions on Affective Computing* 12, no. 3 (2020): 595-606.
- [10] Mollahosseini, Ali, Behzad Hasani, and Mohammad H. Mahoor. "Affectnet: A database for facial expression, valence, and arousal computing in the wild." *IEEE Transactions on Affective Computing* 10, no. 1 (2017): 18-31.
- [11] C. Mühl, B. Allison, A. Nijholt, G. Chanel, A survey of affective brain computer interfaces: principles, state-of-the-art, and challenges, *Brain-Computer Interfaces* 1 (2) (2014) 66–84.
- [12] S. D'mello, J. Kory, A Review and Meta-Analysis of Multimodal Affect Detection .
- [13] Wang, Dan, and Yi Shang. "Modeling physiological data with deep belief networks." *International journal of information and education technology (IJJET)* 3, no. 5 (2013): 505.
- [14] Miranda, J., M. Khomami Abadi, N. Sebe, and I. Patras. "Amigos: A dataset for mood, personality and affect research on individuals and groups." *IEEE T Affect Comput* (2017): 02.
- [15] Koelstra, Sander, and Ioannis Patras. "Fusion of facial expressions and EEG for implicit affective tagging." *Image and Vision Computing* 31, no. 2 (2013): 164-174.
- [16] Ferdinando, Hany, Tapio Seppänen, and Esko Alasaarela. "Comparing features from ECG pattern and HRV analysis for emotion recognition system." In 2016 IEEE Conference on Computational Intelligence in Bioinformatics and Computational Biology (CIBCB), pp. 1-6. IEEE, 2016.
- [17] Ferdinando, Hany, Liang Ye, Tapio Seppänen, and Esko Alasaarela. "Emotion recognition by heart rate variability." *Australian Journal of Basic and Applied Science* 8, no. 14 (2014): 50-55.
- [18] Vaswani, Ashish, Noam Shazeer, Niki Parmar, Jakob Uszkoreit, Llion Jones, Aidan N. Gomez, Łukasz Kaiser, and Illia Polosukhin. "Attention is all you need." *Advances in neural information processing systems* 30 (2017).
- [19] Le, Hoai-Duy, Guee-Sang Lee, Soo-Hyung Kim, Seungwon Kim, and Hyung-Jeong Yang. "Multi-Label Multimodal Emotion Recognition With Transformer-Based Fusion and Emotion-Level Representation Learning." *IEEE Access* 11 (2023): 14742-14751.
- [20] Mocanu, Bogdan, Ruxandra Tapu, and Titus Zaharia. "Multimodal emotion recognition using cross modal audio-video fusion with attention and deep metric learning." *Image and Vision Computing* (2023): 104676.
- [21] Yu, Jianfei, Kai Chen, and Rui Xia. "Hierarchical interactive multimodal transformer for aspect-based multimodal sentiment analysis." *IEEE Transactions on Affective Computing* (2022).
- [22] Tang, Zineng, Jaemin Cho, Yixin Nie, and Mohit Bansal. "TVLT: Textless Vision-Language Transformer." *arXiv preprint arXiv:2209.14156* (2022).
- [23] Wang, Zhe, Yongxiong Wang, Chuanfei Hu, Zhong Yin, and Yu Song. "Transformers for EEG-based emotion recognition: A hierarchical spatial information learning model." *IEEE Sensors Journal* 22, no. 5 (2022): 4359-4368.
- [24] Song, Rencheng, Senle Zhang, Chang Li, Yunfei Zhang, Juan Cheng, and Xun Chen. "Heart rate estimation from facial videos using a spatiotemporal representation with convolutional neural networks." *IEEE Transactions on Instrumentation and Measurement* 69, no. 10 (2020): 7411-7421.
- [25] Niu, Xuesong, Hu Han, Shiguang Shan, and Xilin Chen. "Synrhythm: Learning a deep heart rate estimator from general to specific." In 2018 24th International Conference on Pattern Recognition (ICPR), pp. 3580-3585. IEEE, 2018.
- [26] Hsu, Gee-Sern, ArulMurugan Ambikapathi, and Ming-Shiang Chen. "Deep learning with time-frequency representation for pulse estimation from facial videos." In 2017 IEEE international joint conference on biometrics (IJCB), pp. 383-389. IEEE, 2017.
- [27] Lu, Hao, Hu Han, and S. Kevin Zhou. "Dual-gan: Joint bvp and noise modeling for remote physiological measurement." In *Proceedings of the IEEE/CVF Conference on Computer Vision and Pattern Recognition*, pp. 12404-12413. 2021.
- [28] Khare, Smith K., and Varun Bajaj. "Time-frequency representation and convolutional neural network-based emotion recognition." *IEEE transactions on neural networks and learning systems* 32, no. 7 (2020): 2901-2909.
- [29] Gasparini, Francesca, Alessandra Grossi, and Stefania Bandini. "A deep learning approach to recognize cognitive load using ppg signals." In *The 14th Pervasive Technologies Related to Assistive Environments Conference*, pp. 489-495. 2021.
- [30] Liang, Yongbo, Zhencheng Chen, Rabab Ward, and Mohamed Elgendi. "Photoplethysmography and deep learning: enhancing hypertension risk stratification." *Biosensors* 8, no. 4 (2018): 101.
- [31] Soleymani, Mohammad, Jeroen Lichtenauer, Thierry Pun, and Maja Pantic. "A multimodal database for affect recognition and implicit tagging." *IEEE transactions on affective computing* 3, no. 1 (2011): 42-55.
- [32] Koelstra, Sander, Christian Muhl, Mohammad Soleymani, Jong-Seok Lee, Ashkan Yazdani, Touradj Ebrahimi, Thierry Pun, Anton Nijholt, and Ioannis Patras. "Deap: A database for emotion analysis; using physiological signals." *IEEE transactions on affective computing* 3, no. 1 (2011): 18-31.
- [33] Russell, James A. "A circumplex model of affect." *Journal of personality and social psychology* 39, no. 6 (1980): 1161.
- [34] Yu, Sung-Nien, Shao-Wei Wang, and Yu Ping Chang. "Improving Distinguishability of Photoplethysmography in Emotion Recognition Using Deep Convolutional Generative Adversarial Networks." *IEEE Access* 10 (2022): 119630-119640.
- [35] Ismail, Sharifah Noor Masidayu Sayed, Nor Azlina Ab Aziz, and Siti Zainab Ibrahim. "A comparison of emotion recognition system using electrocardiogram (ECG) and photoplethysmogram (PPG)." *Journal of King Saud University-Computer and Information Sciences* 34, no. 6 (2022): 3539-3558.
- [36] Lee, M.S., Lee, Y.K., Pae, D.S., Lim, M.T., Kim, D.W. and Kang, T.K., 2019. Fast emotion recognition based on single pulse PPG signal with convolutional neural network. *Applied Sciences*, 9(16), p.3355.
- [37] Sepúlveda, A., Castillo, F., Palma, C. and Rodríguez-Fernández, M., 2021. Emotion recognition from ECG signals using wavelet scattering and machine learning. *Applied Sciences*, 11(11), p.4945.
- [38] Sarkar, P. and Etemad, A., 2020. Self-supervised ECG representation learning for emotion recognition. *IEEE Transactions on Affective Computing*, 13(3), pp.1541-1554.
- [39] Mellouk, W. and Handouzi, W., 2023. CNN-LSTM for automatic emotion recognition using contactless photoplethysmographic signals. *Biomedical Signal Processing and Control*, 85, p.104907.
- [40] Ali, K. and Hughes, C.E., 2021, January. Facial expression recognition by using a disentangled identity-invariant expression representation. In 2020 25th International Conference on Pattern Recognition (ICPR) (pp. 9460-9467). IEEE.
- [41] Li, H., Wang, N., Yang, X., Wang, X. and Gao, X., 2022. Towards semi-supervised deep facial expression recognition with an adaptive confidence margin. In *Proceedings of the IEEE/CVF conference on computer vision and pattern recognition* (pp. 4166-4175).
- [42] Wang, H., Li, B., Wu, S., Shen, S., Liu, F., Ding, S. and Zhou, A., 2023. Rethinking the Learning Paradigm for Dynamic Facial Expression Recognition. In *Proceedings of the IEEE/CVF Conference on Computer Vision and Pattern Recognition* (pp. 17958-17968).
- [43] Lo, L., Ruan, B.K., Shuai, H.H. and Cheng, W.H., 2023. Modeling Uncertainty for Low-Resolution Facial Expression Recognition. *IEEE Transactions on Affective Computing*.

- [44] Ali, K. and Hughes, C.E., 2020. Face reenactment based facial expression recognition. In *Advances in Visual Computing: 15th International Symposium, ISVC 2020, San Diego, CA, USA, October 5-7, 2020, Proceedings, Part I* 15 (pp. 501-513). Springer International Publishing.
- [45] Russell, J.A., 1980. A circumplex model of affect. *Journal of personality and social psychology*, 39(6), p.1161.
- [46] Thayer, R.E., 1990. *The biopsychology of mood and arousal*. Oxford University Press.
- [47] Gunes, H. and Pantic, M., 2010. Automatic, dimensional and continuous emotion recognition. *International Journal of Synthetic Emotions (IJSE)*, 1(1), pp.68-99.
- [48] Kollias, D. and Zafeiriou, S., 2018. A multi-component CNN-RNN approach for dimensional emotion recognition in-the-wild. *arXiv preprint arXiv:1805.01452*.
- [49] Deng, D., Chen, Z. and Shi, B.E., 2020, November. Multitask emotion recognition with incomplete labels. In *2020 15th IEEE International Conference on Automatic Face and Gesture Recognition (FG 2020)* (pp. 592-599). IEEE.
- [50] Kuhnke, F., Rumberg, L. and Ostermann, J., 2020, November. Two-stream aural-visual affect analysis in the wild. In *2020 15th IEEE International Conference on Automatic Face and Gesture Recognition (FG 2020)* (pp. 600-605). IEEE.
- [51] Zhang, Y.H., Huang, R., Zeng, J. and Shan, S., 2020, November. M3f: Multi-modal continuous valence-arousal estimation in the wild. In *2020 15th IEEE International Conference on Automatic Face and Gesture Recognition (FG 2020)* (pp. 632-636). IEEE.
- [52] Zeng, Z., Pantic, M. and Huang, T.S., 2009. Emotion recognition based on multimodal information. In *Affective information processing* (pp. 241-265). London: Springer London.
- [53] Yin, Z., Zhao, M., Wang, Y., Yang, J. and Zhang, J., 2017. Recognition of emotions using multimodal physiological signals and an ensemble deep learning model. *Computer methods and programs in biomedicine*, 140, pp.93-110.
- [54] Katsigiannis, S. and Ramzan, N., 2017. DREAMER: A database for emotion recognition through EEG and ECG signals from wireless low-cost off-the-shelf devices. *IEEE journal of biomedical and health informatics*, 22(1), pp.98-107.
- [55] Santamaria-Granados, L., Munoz-Organero, M., Ramirez-Gonzalez, G., Abdulhay, E. and Arunkumar, N.J.I.A., 2018. Using deep convolutional neural network for emotion detection on a physiological signals dataset (AMIGOS). *IEEE Access*, 7, pp.57-67.
- [56] Elalamy, R., Fanourakis, M. and Chanel, G., 2021, September. Multi-modal emotion recognition using recurrence plots and transfer learning on physiological signals. In *2021 9th International Conference on Affective Computing and Intelligent Interaction (ACII)* (pp. 1-7). IEEE.
- [57] Soleymani, M., Asghari-Esfeden, S., Fu, Y. and Pantic, M., 2015. Analysis of EEG signals and facial expressions for continuous emotion detection. *IEEE Transactions on Affective Computing*, 7(1), pp.17-28.
- [58] Wang, S., Qu, J., Zhang, Y. and Zhang, Y., 2023. Multimodal Emotion Recognition From EEG Signals and Facial Expressions. *IEEE Access*, 11, pp.33061-33068.
- [59] de Souza Neto, E.P., Custaud, M.A., Frutoso, J., Somody, L., Gharib, C. and Fortrat, J.O., 2001. Smoothed pseudo Wigner-Ville distribution as an alternative to Fourier transform in rats. *Automatic Neuroscience*, 87(2-3), pp.258-267.
- [60] Scholl, Stefan. "Fourier, Gabor, Morlet or Wigner: comparison of time-frequency transforms." *arXiv preprint arXiv:2101.06707* (2021).
- [61] Antoine, J-P, Pierre Carrette, Romain Murenzi, and Bernard Piette. "Image analysis with two-dimensional continuous wavelet transform." *Signal processing* 31, no. 3 (1993): 241-272.
- [62] He, Kaiming, Xiangyu Zhang, Shaoqing Ren, and Jian Sun. "Deep residual learning for image recognition." In *Proceedings of the IEEE conference on computer vision and pattern recognition*, pp. 770-778. 2016.
- [63] He, K., Chen, X., Xie, S., Li, Y., Dollár, P. and Girshick, R., 2022. Masked autoencoders are scalable vision learners. In *Proceedings of the IEEE/CVF conference on computer vision and pattern recognition* (pp. 16000-16009).
- [64] Tan, Hao, and Mohit Bansal. "Lxmert: Learning cross-modality encoder representations from transformers." *arXiv preprint arXiv:1908.07490* (2019).
- [65] Lu, Jiasen, Dhruv Batra, Devi Parikh, and Stefan Lee. "Vilbert: Pretraining task-agnostic visiolinguistic representations for vision-and-language tasks." *Advances in neural information processing systems* 32 (2019).
- [66] Kim, Wonjae, Bokyung Son, and Ildoo Kim. "Vilt: Vision-and-language transformer without convolution or region supervision." In *International Conference on Machine Learning*, pp. 5583-5594. PMLR, 2021.
- [67] Chen, Yen-Chun, Linjie Li, Licheng Yu, Ahmed El Kholy, Faisal Ahmed, Zhe Gan, Yu Cheng, and Jingjing Liu. "Uniter: Learning universal image-text representations." (2019).
- [68] Zadeh, AmirAli Bagher, Paul Pu Liang, Soujanya Poria, Erik Cambria, and Louis-Philippe Morency. "Multimodal language analysis in the wild: Cmu-mosei dataset and interpretable dynamic fusion graph." In *Proceedings of the 56th Annual Meeting of the Association for Computational Linguistics (Volume 1: Long Papers)*, pp. 2236-2246. 2018.
- [69] Wu, Yi-Chiao, Li-Wen Chiu, Chun-Chih Lai, Bing-Fei Wu, and Sunny SJ Lin. "Recognizing, Fast and Slow: Complex Emotion Recognition with Facial Expression Detection and Remote Physiological Measurement." *IEEE Transactions on Affective Computing* (2023).
- [70] Liu, Xin, Josh Fromm, Shwetak Patel, and Daniel McDuff. "Multi-task temporal shift attention networks for on-device contactless vitals measurement." *Advances in Neural Information Processing Systems* 33 (2020): 19400-19411.
- [71] Yu, Zitong, Wei Peng, Xiaobai Li, Xiaopeng Hong, and Guoying Zhao. "Remote heart rate measurement from highly compressed facial videos: an end-to-end deep learning solution with video enhancement." In *Proceedings of the IEEE/CVF International Conference on Computer Vision*, pp. 151-160. 2019.
- [72] Kingma, Diederik P., and Jimmy Ba. "Adam: A method for stochastic optimization." *arXiv preprint arXiv:1412.6980* (2014).
- [73] Ilya Loshchilov and Frank Hutter. "Decoupled weight decay regularization". In *ICLR*, 2019.
- [74] Yoon, Hyun Joong, and Seong Youb Chung. "EEG-based emotion estimation using Bayesian weighted-log-posterior function and perceptron convergence algorithm." *Computers in biology and medicine* 43, no. 12 (2013): 2230-2237.
- [75] Atkinson, John, and Daniel Campos. "Improving BCI-based emotion recognition by combining EEG feature selection and kernel classifiers." *Expert Systems with Applications* 47 (2016): 35-41.
- [76] Yu, Zitong, Xiaobai Li, and Guoying Zhao. "Remote photoplethysmograph signal measurement from facial videos using spatio-temporal networks." *arXiv preprint arXiv:1905.02419* (2019).
- [77] Zhang, Kaipeng, Zhanpeng Zhang, Zhifeng Li, and Yu Qiao. "Joint face detection and alignment using multitask cascaded convolutional networks." *IEEE signal processing letters* 23, no. 10 (2016): 1499-1503.

Kamran Ali Kamran Ali is a postdoctoral research associate in the computer science department at the University of Central Florida, Orlando, FL, 32816, USA. His research interests include computer vision and machine learning. He is the corresponding author of this article. Contact him at kamran.ali@ucf.edu.



Charles E. Hughes Charles E. Hughes is a pegasus professor of Computer Science at the University of Central Florida, Orlando, FL, 32816, USA. His research interests include virtual learning environments, computer graphics, machine learning, and visual programming systems. Contact him at charles.hughes@ucf.edu.